Population and Phase Coherence during the Growth of an Elongated Bose-Einstein Condensate

M. Hugbart, J. A. Retter, A. F. Varón, P. Bouyer,* and A. Aspect
Laboratoire Charles Fabry de l'Institut d'Optique,
Centre National de la Recherche Scientifique et Université Paris Sud 11,
Batiment 503, Centre Scientifique F91403 ORSAY CEDEX, France.

M. J. Davis
ARC Centre of Excellence for Quantum-Atom Optics, School of Physical Sciences,
University of Queensland, Brisbane, QLD 4072, Australia.

(Dated: May 29, 2006)

We study the growth of an elongated phase-fluctuating condensate from a non-equilibrium thermal cloud obtained by shock-cooling. We compare the growth of the condensate with numerical simulations, revealing a time delay and a reduction in the growth rate which we attribute to phase fluctuations. We measure the phase coherence using momentum Bragg spectroscopy, and thereby observe the evolution of the phase coherence as a function of time. Combining the phase coherence results with the numerical simulations, we suggest a simple model for the reduction of the growth rate based on the reduction of bosonic stimulation due to phase fluctuations and obtain improved agreement between theory and experiment.

The non-equilibrium path to Bose-Einstein condensation is a complex process in which atoms accumulate in the ground state of the system and long-range phase coherence develops, resulting in a strong suppression of density fluctuations and a uniform phase. The kinetics of condensate formation has long been a subject of theoretical study, giving rise to a number of conflicting predictions (see [1] for a review). Quantitative theories have been formulated to model the condensate formation process in a harmonic trapping potential [2, 3]. However, a limitation of these models is that the condensate is assumed to grow adiabatically in its phase coherent ground state. On the other hand, for a homogeneous system, Kagan *et al.* [4] proposed the appearance of a quasi-condensate with strong phase fluctuations which die out on a time scale that increases with the size of the system. This homogeneous system description is also relevant to condensate growth in hydrodynamic clouds, where the trapping potential can be neglected [5]. Condensates in highly-elongated traps, which can often be treated using the local density approximation, are expected to have properties close to the homogeneous case [6]. In addition, the axially hydrodynamic regime is easily attainable in such traps [7].

Experimentally, the problem of condensate formation has been approached by shock-cooling [8, 9, 10] in harmonic traps: starting from a thermal cloud just above the transition temperature, rapid removal of the most energetic atoms from the trap results in an over-saturated thermal cloud. Subsequent thermalization leads to the growth of the condensate. Measurements of the growth of the condensed fraction in traps significantly less elongated than ours [8, 9] have obtained good quantitative agreement with theory [9, 11], but these experiments did not give access to the phase coherence of the growing condensate. Although the two-step growth curve reported in Ref. [9], and the growth of non-equilibrium, phase-fluctuating condensates from hydrodynamic clouds in Ref. [10] support the existence of a quasi-condensate during the initial stage of condensate formation as proposed in Ref. [4], there exists to our knowledge no quantitative experimental study of the development of phase coherence.

In this Letter we present an experimental study of the evolution of both the condensate number and the phase coherence during the growth of a condensate in a highly elongated trap in the axially hydrodynamic regime. We observe that the growth is slower than that predicted by theory and attribute this to the presence of phase fluctu-

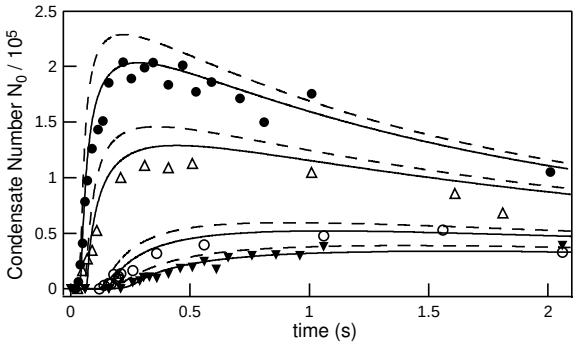

FIG. 1: Condensate growth curves for initial atom numbers: $N_i/10^5 = 8.6(9)\bullet$, $7.2(7)\triangle$, $3.4(4)\circ$ and $2.8(5)\blacktriangledown$ [20]. Each point corresponds to an average over three experimental realizations. The solid (dashed) lines are theoretical results of the model of [11], with (without) the correction for thermal phase fluctuations, as described in the text. They have additional delay times of 10, 20, 50, and 50 ms respectively. The decrease in N_0 at longer times is due to three-body losses.

ations which are expected to be strong in our experimental regime, even at equilibrium [6]. We then use Bragg spectroscopy [12, 13] to measure the coherence length during the growth of the condensate. Our observations are compatible with the scenario of Refs. [4, 5], where a non-equilibrium quasi-condensate is created at the onset of condensation and relaxes rapidly to equilibrium with shape oscillations. Finally, we propose a simple modification to the numerical simulations to phenomenologically account for the effect of phase fluctuations on the condensate growth rate, and find that this improves the agreement between theory and experiment.

In our experiment [14], we prepare a thermal cloud of ^{87}Rb atoms in the $5S_{1/2}|F = 1, m_F = -1\rangle$ state in an Ioffe-Pritchard trap with final trap frequencies of $\omega_\perp = 2\pi\times 655(4)$ Hz radially and $\omega_z = 2\pi\times 6.53(1)$ Hz axially. Forced radio-frequency (rf) evaporation proceeds to a frequency $\Delta\nu_{\rm rf} = 140$ kHz above that corresponding to the bottom of the combined magnetic and gravitational potential, giving an effective trap depth of $\varepsilon_{\rm i} = 6$ μK, and the rf knife is held at this value for a time varying from 1 s to 12 s. This ensures thermal equilibrium, and allows us to control the atom number $N_{\rm i}$ in the range 2.7–8.6×10^5. The resulting thermal cloud has a temperature $T_{\rm i}$ of about $\varepsilon_{\rm i}/10$, just above the transition temperature $T_{\rm c}$, which varies from 400 nK to 600 nK depending on the atom number.

We next shock-cool the cloud by rapidly ramping the rf knife to $\Delta\nu_{\rm rf} = 40$ kHz in 25 ms, giving a final trap depth $\varepsilon_{\rm f} = 1.5$ μK. The relative truncation rate $\dot{\varepsilon}/\varepsilon_{\rm f} = 120$ s^{-1} is fast compared to the axial trap frequency, but slow compared to the radial trap frequency. In our elongated geometry this shock-cooling results in a cloud transversally at equilibrium but axially out of equilibrium. The cloud tends towards local thermal equilibrium with a temperature $T < T_{\rm c}$, in a time $\sim 3\,\tau_{\rm coll} \lesssim 10$ ms [15] where $\tau_{\rm coll}$ is the collision rate at the centre of the trap [16]. Since the atom cloud is in the hydrodynamic regime axially ($\omega_z\tau_{\rm coll} \ll 1$) [17], global equilibrium is reached on a time scale longer than the axial oscillation period.

In order to study the condensate growth, the cloud is held in the trap for a further time t after the end of the shock-cooling ramp, with the trap depth held constant at $\varepsilon_{\rm f}$. We then switch off the trap and image the cloud after a 20 ms time-of-flight in order to obtain the total atom number N, temperature T and condensate number N_0 [7, 18]. By repeating the measurements at different times t for the same initial conditions, we obtain a growth curve for the condensate number, as shown in Fig. 1 for various initial atom numbers $N_{\rm i}$ [20]. At $t \simeq 20$ ms (depending on initial conditions), the atom number has dropped by 40% and the temperature is already below $T_{\rm c}$, yet the condensate does not appear until later, with a delay time of 20–200 ms after the fast ramp.

We have simulated the evaporative cooling and condensate growth for our experiment based on the model described in [11] with the additional inclusion of three-body loss for the thermal cloud [19]. The results are shown in Fig. 1 (dashed lines). This method was in good quantitative agreement with experimental results for a less-elongated system [9]. There are no free parameters in our calculations which are based on our measured data [20], however the results plotted in Fig. 1 (dashed lines) have had a delay time of 10–50 ms added to better fit the experimental results. The observed growth rate is somewhat slower than the theoretical prediction. However, the simulation is not necessarily valid for such an elongated system, in the hydrodynamic regime, nor does it take account of phase fluctuations. Indeed, our experiment is performed in an elongated trapping geometry, where temperature-dependent phase-fluctuations can be present even at equilibrium [6, 13, 21, 22, 23]. For our parameters, the phase-coherence length $L_\phi = 15\hbar^2 N_0/16mk_{\rm B}LT$ [6] at equilibrium is smaller than the condensate half-length L by a factor in the range 4–10, varying inversely with the condensate atom number. We will return to this point in more detail after discussing our experimental study of the phase coherence.

We measure the coherence length of the condensate during its formation via its momentum distribution, using 4-photon Bragg Spectroscopy as described in Ref. [13]. At time t after the end of the shock-cooling ramp, the magnetic trap is switched off and after 2 ms of free expansion a 2 ms Bragg pulse is applied. The atoms are imaged after a further 16 ms time-of-flight, which allows separation of the diffracted atoms. The diffracted fraction is measured as a function of ν, the detuning between the Bragg beams which determines the

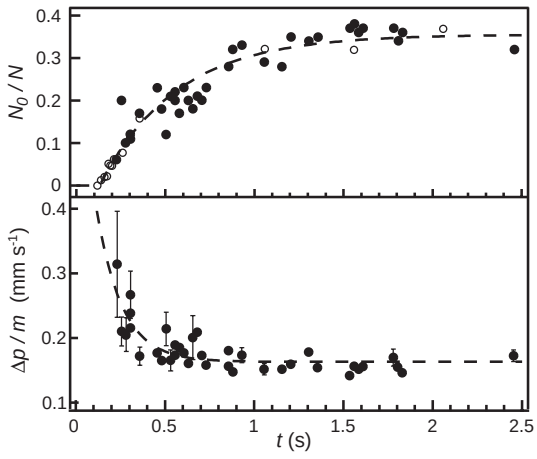

FIG. 2: Condensed fraction N_0/N and momentum width Δp as a function of t for an initial atom number $N_{\rm i} = 3.8(3)\times10^5$. (Open circles correspond to the data from Fig. 1 for $N_{\rm i} = 3.4(3)\times10^5$.) The decreasing momentum width indicates the growth of the coherence length with time. The dashed lines are guides to the eye. Some typical error bars are shown.

velocity-class diffracted, to obtain the momentum spectrum of the condensate. We fit a Lorentzian function to the measured spectra and extract the half-width at half-maximum (HWHM) $\Delta\nu = 2k_{\rm L}\Delta p/2\pi m$, where m is the atomic mass, $k_{\rm L}$ the laser wave-vector and Δp the HWHM of the momentum distribution. For each spectrum, further images (typically 5) are taken without the Bragg pulses, from which the temperature T, condensate number N_0, and condensate half-length L are obtained.

The evolution of the momentum width Δp for an initial atom number $N_{\rm i} = 3.8(3)\times 10^5$ is presented in Fig. 2 (lower panel). The corresponding condensed fractions are shown in the upper panel of Fig. 2 (filled circles). The momentum width Δp clearly decreases as the condensate fraction grows to equilibrium, indicating that, as expected, the coherence length grows with time. Indeed, for a condensate at equilibrium, we know [13] that the reduction in coherence length due to thermal phase fluctuations leads to a broadening of the momentum width, given by [6, 24]:

$$\Delta p_{\rm equ} = \hbar\sqrt{\left(\frac{2.04}{L}\right)^2 + \left(\frac{0.65}{L_\phi}\right)^2}. \qquad (1)$$

The first term accounts for the Heisenberg-limited momentum width due to the finite size L of the condensate and the second term accounts for the presence of thermal phase fluctuations. The numerical factors account for integration over the 3D density profile. We also correct for the finite "instrumental width" of the Bragg spectrometer, by introducing as in [13] a Gaussian apparatus function of half-width $w_{\rm G} = 200$ Hz. This results in a theoretical momentum width: $\Delta p_{\rm th} = \Delta p_{\rm equ}/2 + \sqrt{(2\pi m/2k_{\rm L})^2\, w_{\rm G}^2 + (\Delta p_{\rm equ}/2)^2}$. Equation 1 shows that, even if the condensate were at equilibrium at each instant during the growth, we would expect the momentum width to decrease with time, since both L_ϕ and L increase with the condensate atom number. We can therefore test whether the condensate coherence follows the density in this way by comparing each measured momentum width Δp with the value $\Delta p_{\rm th}$ calculated for a condensate at equilibrium, using the parameters N_0, L and T measured for each Bragg spectrum. We plot the ratio $\Delta p/\Delta p_{\rm th}$ in Fig. 3 for two different initial atom numbers. The dashed line at $\Delta p/\Delta p_{\rm th} = 1$ indicates the value expected for a condensate always at equilibrium. Systematic uncertainties of 15% on this equilibrium value, mainly due to the atom number calibration (20%) and determination of $w_{\rm G}$ (10%), are represented by the gray band. Unambiguously, we observe that the ratio $\Delta p/\Delta p_{\rm th}$ always lies above one (dashed line), and decreases in time. This indicates an excess momentum spread with respect to a condensate at equilibrium during the growth. As the condensate reaches equilibrium, the measurement dispersion decays and the momentum width tends to the predicted equilibrium value.

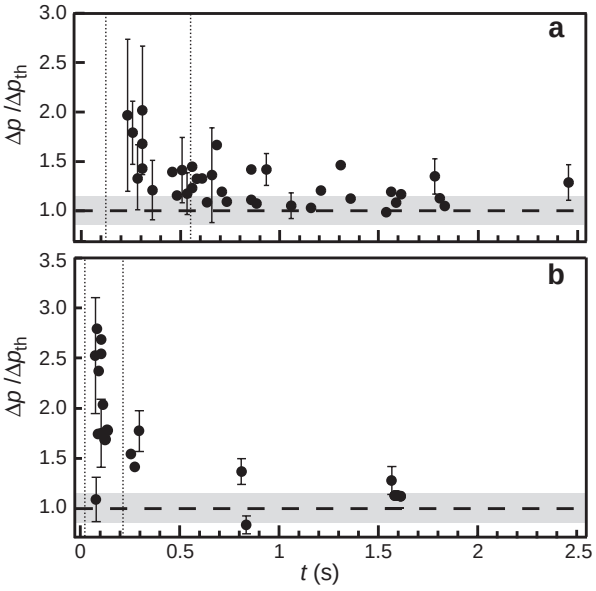

FIG. 3: Ratio of measured momentum width Δp to theoretical momentum width $\Delta p_{\rm th}$, calculated for a condensate at equilibrium (see text) for: (a) $N_{\rm i} = 3.8(3)\times 10^5$ and (b) $N_{\rm i} = 7.2(3)\times 10^5$. (Data shown in (a) corresponds to Fig. 2.) The condensate momentum width tends to the equilibrium value (dashed line) at long times. Some typical statistical error bars are shown; the gray band indicates systematic uncertainties on the equilibrium value. The first vertical line marks the onset of condensation; the second indicates the time at which the condensed fraction reaches $(1 - 1/e)$ of its final value.

To interpret our results, we consider the scenario proposed by Kagan *et al.* [4] for condensate growth in a homogeneous system. The early stages of growth lead to a quasi-condensate with non-equilibrium, long-range phase fluctuations in which density fluctuations are suppressed. The phase-fluctuations then decay to produce the true phase-coherent condensate, with a characteristic time scale τ_ϕ which increases with the system size L: $\tau_\phi \propto L$ in the collisionless regime and $\tau_\phi \propto L^2$ in the hydrodynamic regime. Although our trapped system differs from the homogeneous system considered in Ref. [4], Svistunov [5] points out that this theory can be applied to trapped hydrodynamic clouds, where the trapping potential can be neglected. In this case, the resulting quasi-condensate will be out-of-equilibrium with respect to a global coherent motion in the trap, thereby exciting a quadrupole mode similar to that observed in Refs. [10, 13]. Indeed, for a higher atom number $N_{\rm i} = 8.6\times 10^5$ we directly observe quadrupole oscillations, with an amplitude (in the trap) of 12 μm and a decay constant of about 250 ms. Oscillations of the axial condensate length broaden the momentum distribution, thus the excess momentum widths in Fig. 3 can be attributed to quadrupole oscillations with amplitudes of 4 μm ($N_{\rm i} = 3.8\times 10^5$) and 5.5 μm ($N_{\rm i} = 7.2\times 10^5$) [25]

and decay constants of about 700 ms and 300 ms respectively. These values are consistent with those obtained for $N_{\rm i} = 8.6 \times 10^5$, assuming an oscillation amplitude and decay rate which increase with the atom number. Therefore, apart from this decaying quadrupole mode, we conclude that higher-order, non-equilibrium phase fluctuations have decayed within a time shorter than 100 ms after the onset of condensation, in qualitative agreement with the predictions of Kagan *et al.* [26].

This result allows us to interpret the data of Fig. 1, where the observed growth is slower than that predicted for a phase-coherent condensate. We suggest a simple picture of a 1D phase-fluctuating condensate as being made up of a number of phase-coherent domains. As the growth rate includes a factor $(1+N_0)$ due to bosonic stimulation, the growth rate of each domain will be smaller than that of a single large condensate, thereby reducing the overall growth rate. We have shown that the coherence length of our condensate approximately follows the equilibrium prediction, L_ϕ, which can be calculated using the instantaneous values of N_0, L and T measured during the observed growth. We therefore modify the growth rate in the simulation, replacing the factor $1 + N_0$ with $1 + L_\phi N_0/L$ [27]. This slows the simulated growth rate, obtaining improved agreement with the data as shown by the solid lines in Fig. 1 [20]. However, the added delay time remains unexplained.

In conclusion, we have observed the growth of a condensate in an elongated trap and have shown, by comparison with numerical simulations, that the presence of phase fluctuations slows the growth of the condensed fraction. By studying the evolution of the momentum width during condensate growth, we have directly observed the growth of the phase coherence with time. Compared with that expected for a condensate at equilibrium, these measurements reveal a broadening of the momentum distribution during growth, compatible with quadrupole shape oscillations. Apart from this decaying oscillation, we conclude that the condensate has already reached the equivalent equilibrium coherence length within 100 ms after the onset of condensation. Because a complete theory for our experimental situation is lacking, the agreement between theory and experiment can only be qualitative and an extension of the model of Ref. [4] to trapped condensates, particularly in this quasi-1D geometry [28], is required.

Using the equilibrium coherence length, we accurately predict the slowing of the growth rate due to phase fluctuations. However, there remains a discrepancy on the delay time before condensation, which may indicate non-equilibrium excitations at early times, as predicted by Ref. [4]. A measurement of the phase coherence length at shorter times is needed. This is exceedingly difficult in our system, since at short times the condensed fraction is too small to obtain clear Bragg spectra. Other techniques might be used instead, such as atom laser correlation measurements [29], combined with single-atom detection [30, 31].

We thank L. Sanchez-Palencia, G. V. Shlyapnikov, F. Gerbier, S. Richard and J. H. Thywissen for useful discussions. We acknowledge support from IXSEA (M.H.), the Marie Curie Fellowship Programme (J.R.), the Fundación Mazda para el Arte y la Ciencia (A.V), the Australian Research Council (M.D.), the Délégation Générale de l'Armement, the Ministère de la Recherche (ACI Nanoscience 201), the European Union (grants IST-2001-38863 and MRTN-CT-2003-505032) and the ESF (QUDEDIS programme). The atom optics group of the Laboratoire Charles Fabry is a member of IFRAF (www.ifraf.org).

* Electronic address: philippe.bouyer@iota.u-psud.fr

[1] H. T. C. Stoof, J. Low Temp. Phys. **114**, 11 (1999).
[2] C. W. Gardiner, P. Zoller, R. J. Ballagh, and M. J. Davis, Phys. Rev. Lett **79**, 1793 (1997); M. D. Lee and C. W. Gardiner, Phys. Rev. A **62**, 033606 (2000); M. J. Davis, C. W. Gardiner, and R. J. Ballagh, *ibid* **62**, 063608 (2000).
[3] M. J. Bijlsma, E. Zaremba, and H. T. C. Stoof, Phys. Rev. A **62**, 063609 (2000).
[4] Yu. Kagan, B. V. Svistunov, and G. V. Shlyapnikov, JETP **75**, 387 (1992); Yu. Kagan and B. V. Svistunov, *ibid* **78**, 187 (1994); Yu. Kagan and B. V. Svistunov, Phys. Rev. Lett. **79**, 3331 (1997).
[5] B. Svistunov, Phys. Lett. A **287**, 169 (2001).
[6] D. S. Petrov, G. V. Shlyapnikov, and J. T. M. Walraven, Phys. Rev. Lett. **87**, 050404 (2001).
[7] F. Gerbier *et al*, Phys. Rev. Lett. **92**, 030405 (2004).
[8] H.-J. Miesner *et al.*, Science **279**, 1005 (1998).
[9] M. Köhl *et al.*, Phys. Rev. Lett. **88**, 080402 (2002).
[10] I. Shvarchuck *et al.*, Phys. Rev. Lett **89**, 270404 (2002).
[11] M. J. Davis and C. W. Gardiner, J. Phys. B **35**, 733 (2002).
[12] J. Stenger *et al.*, Phys. Rev. Lett. **82**, 4569 (1999).
[13] S. Richard *et al*, Phys. Rev. Lett. **91**, 010405 (2003).
[14] B. Desruelle *et al*, Phys. Rev. A **60**, R1759 (1999).
[15] C. R. Monroe *et al.*, Phys. Rev. Lett. **70**, 414 (1993); H. Wu and C. J. Foot, J. Phys. B **29**, L321 (1996).
[16] Here, $1/\tau_{\rm coll} = n_0 \sigma_{\rm el} \bar{v}$, where n_0 is the peak atomic density, $\bar{v} = \sqrt{8 k_{\rm B} T/\pi m}$ the thermal velocity and $\sigma_{\rm el} = 8\pi a^2$ the cross-section for elastic scattering, with m the atomic mass and $a = 5.31(1)$ nm the s-wave scattering length [see E. G. M. van Kempen *et al.*, Phys. Rev. Lett. **88**, 093201 (2002)].
[17] For the thermal cloud immediately before the shock-cooling ramp, we obtain $0.04 < \omega_z \tau_{\rm coll} < 0.13$.
[18] F. Gerbier *et al*, Phys. Rev. A **70**, 013607 (2004).
[19] M. J. Davis, in preparation.
[20] All raw measured atom numbers N have been rescaled by a factor 0.9 (consistent with our 20% estimated error) in order to obtain better agreement between experiment and theory.
[21] S. Dettmer *et al.*, Phys. Rev. Lett. **87**, 160406 (2001).
[22] D. Hellweg *et al.*, Phys. Rev. Lett. **91**, 010406 (2003).

[23] M. Hugbart *et al.*, Eur. Phys. J. D **35**, 155 (2005).
[24] F. Gerbier *et al.*, Phys. Rev. A **67**, 051602(R) (2003).
[25] For such small amplitudes, the oscillations cannot be directly observed in the time-of-flight images due to the limited resolution of our imaging system.
[26] With our experimental parameters we calculate from [4] a damping time τ_ϕ between 10 ms and 500 ms, depending on the collisional regime.
[27] Here, we ignore the additional quadrupole oscillations.
[28] N. P. Proukakis, J. Schmiedmayer, and H. T. C. Stoof, Phys. Rev. A **73**, 053603 (2006).
[29] I. Bloch, T. W. Hänsch, and T. Esslinger, Nature **403**, 166 (2000).
[30] A. Öttl, S. Ritter, M. Köhl, and T. Esslinger, Phys. Rev. Lett. **95**, 090404 (2005).
[31] M. Schellekens, *et al.* Science, **310**, 648 (2005).